Fast-Ion Losses due to Externally Applied Static Magnetic Perturbations in the Large Helical Device*)

Kunihiro OGAWA[1)], Mitsutaka ISOBE[1,2)], Kazuo TOI[1)], Akihiro SHIMIZU[1)], Masaki OSAKABE[1)] and LHD Experiment Group[1)]

[1)]*National Institute for Fusion Science, 322-6 Oroshi-cho, Toki 509-5292, Japan*
[2)]*The Graduate University for Advanced Studies (SOKENDAI), Toki 509-5292, Japan*

(Received 26 November 2013 / Accepted 19 May 2014)

In this study, using a scintillator-based lost fast-ion probe, we have measured fast-ion losses in the Large Helical Device, in which the losses were caused by externally applied static magnetic perturbations (MPs) having small amplitudes. Energy and pitch-angle resolved measurements reveal that the effects of MPs on fast-ion losses occur in both high and low pitch-angle regions. A Lorentz orbit-following calculation indicates that static MPs can change the orbits of fast ions, which can enhance the transport/loss of fast ions.

Keywords: fast ion, Large Helical Device, lost-fast ion probe, static magnetic perturbation

DOI: 10.1585/pfr.9.3402097

1. Introduction

In operating fusion devices, one issue is maintaining an acceptable level for the heat load on the first wall or on a divertor. In ITER, the nominal peak divertor plate heat load is expected to be 5 MW/m^2, which is below the acceptable divertor heat load of 10 MW/m^2 [1]. However, the ratio of edge localized mode (ELM) [2] energy losses expected for spontaneous uncontrolled ELMs in $Q = 10$ scenarios to the maximum value required to avoid divertor erosion is predicted to be up to 30 [3]. In tokamaks and helical/stellarator devices, reductions in divertor heat loads due to ELMs have been demonstrated by externally applying static magnetic perturbations (MPs) [4–8]. Such MPs may increase the local heat load of fast ions on the first wall because they break the symmetry of the magnetic field. Recently, to study the effects of externally applied MPs on fast-ion losses, a scintillator-based lost-fast ion probe (SLIP) [9, 10] was applied in the Large Helical Device (LHD). The SLIP gives the distribution of energy (E) and pitch angle (χ) of fast ions that escape from the plasma as functions of time. This work was conducted to clarify the effects of static MPs on fast-ion losses in the LHD. This paper is organized as follows. Section 2 briefly introduces experimental setups on the LHD. Experimental results are presented in Section 3. The orbit-following calculation is described in Section 4. Section 5 summarizes the work.

2. Experimental Setup

The LHD is the largest helical device in the world with the average minor and major radii of 0.60 m and 3.90 m, respectively. Three tangentially injected high energy (up to 180 keV) neutral beam injections (NBIs) are available on the LHD. Those high power NBIs generate fast ions in LHD plasmas. By using these ions, studies on fast-ion confinement and/or losses have been performed [11]. Externally applied static MPs are generated by ten pairs of so-called local island divertor (LID) coils located outside the vacuum vessel of the LHD (Fig. 1). In these experiments, we use SLIP to measure fast-ion losses. A SLIP works as a magnetic spectrometer that simultaneously provides E and χ of lost-fast ions. Illumination images are captured with an image-intensified (I.I.) CMOS camera and by a 4×4 photomultiplier tube (PMT) array. Fast-ion losses are measured at a SLIP position with a major radius $R = 4.62$ m and the height from the midline of the plasma $z = 0.215$ m. The detailed structure and function of the SLIP are described in Refs. 9 and 10. Electron temperature (T_e) and electron density (n_e) profiles are provided by Thomson scattering diagnostics [12]. The line-averaged density ($\langle n_e \rangle$) is measured with a multichannel far-infrared laser interferometer [13].

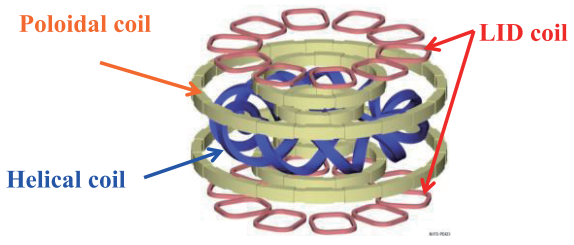

Fig. 1 Coils on the LHD. Ten pairs of LID coils are used to apply MPs to the plasma.

author's e-mail: ogawa.kunihiro@lhd.nifs.ac.jp
*) This article is based on the presentation at the 23rd International Toki Conference (ITC23).

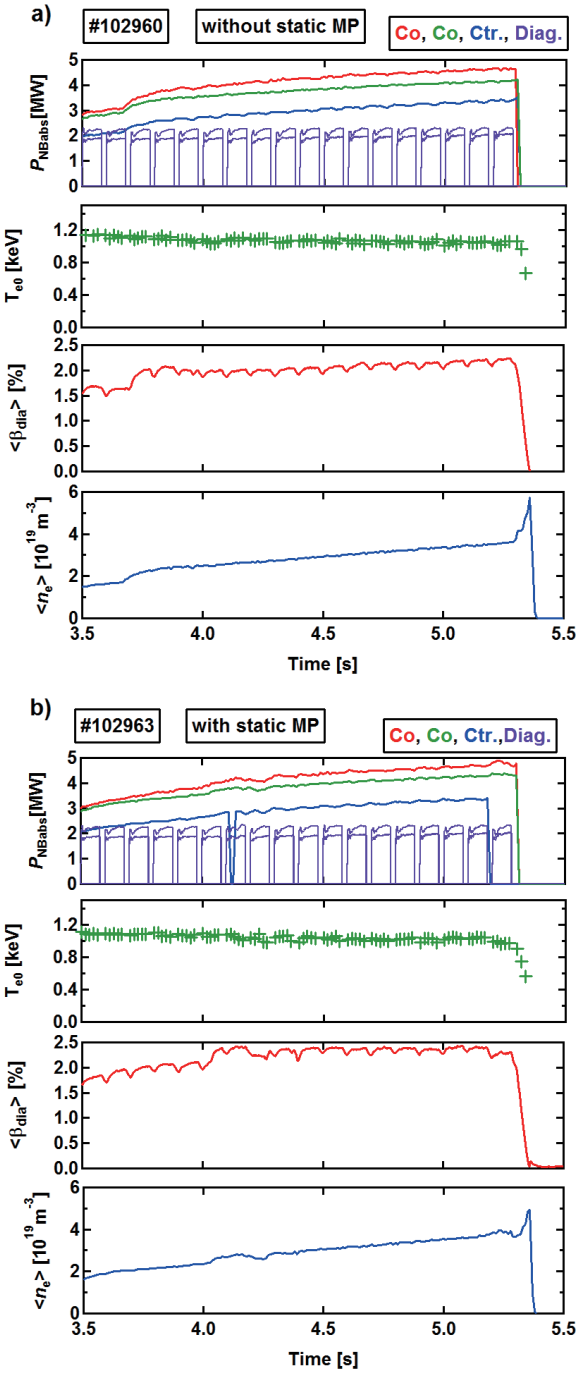

Fig. 2 Time evolution of P_{NBabs}, T_{e0}, $\langle\beta_{\mathrm{dia}}\rangle$, and $\langle n_{\mathrm{e}}\rangle$ for (a) a discharge with no MP and (b) a discharge with MPs.

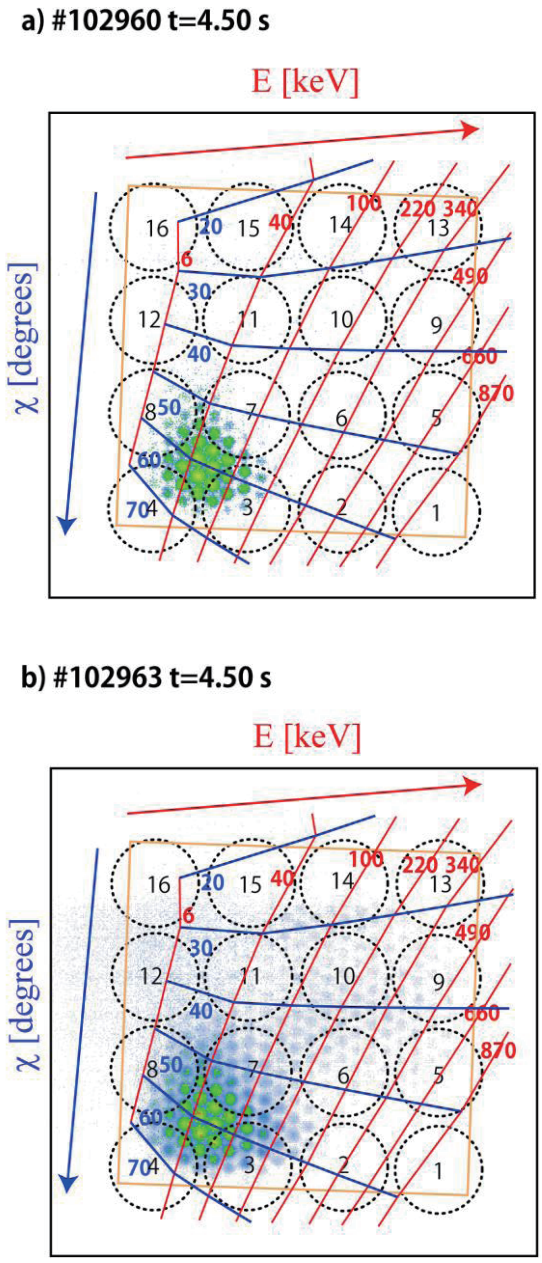

Fig. 3 Scintillation images of SLIP captured by CMOS camera for (a) a discharge with no MP and (b) a discharge with MPs.

3. Experimental Results

Experiments were performed in a magnetic configuration with toroidal magnetic field strength (B_{t}) of 0.9 T (direction of toroidal field is counterclockwise from the top) and a preset magnetic axis position (R_{ax}) of 3.60 m. Figure 2 shows time evolutions of the absorbed power of NB (P_{NBabs}), T_{e} at the plasma center (T_{e0}), volume-averaged plasma beta ($\langle\beta_{\mathrm{dia}}\rangle$), and $\langle n_{\mathrm{e}}\rangle$ in discharges with static MPs (Fig. 2 (a)) and without static MPs (Fig. 2 (b)). In these discharges, diagnostic (Diag.) beams were injected into the plasma. Note that there was no significant difference in global parameters (T_{e0}, $\langle\beta_{\mathrm{dia}}\rangle$, and $\langle n_{\mathrm{e}}\rangle$) of the plasma in these discharges because the amplitudes of the MPs were not large enough to affect global confinement of the plasma; the radial field strength of the static MP on the magnetic axis position was about 10^{-3} T. No static MP was applied in shot number 102960, but in shot number 102963, static MPs having constant amplitude were applied throughout the discharge. Figures 3 (a) and 3 (b) show the scintillation images captured by the CMOS camera of SLIP at 4.50 s in shot number 102960 and 4.50 s in shot number 102963, respectively. The E and χ grids were calculated using the numerical grid map calculation

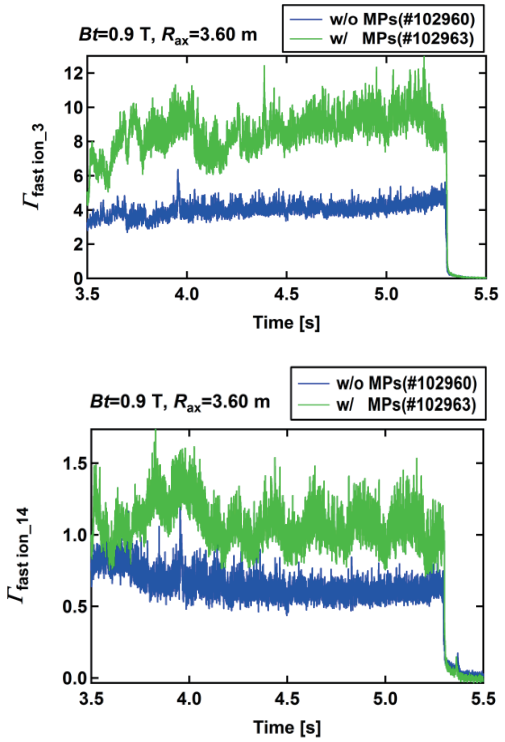

Fig. 4 Time evolutions of fast-ion-loss signals measured by SLIP at PMT 3 (top) and 14 (bottom).

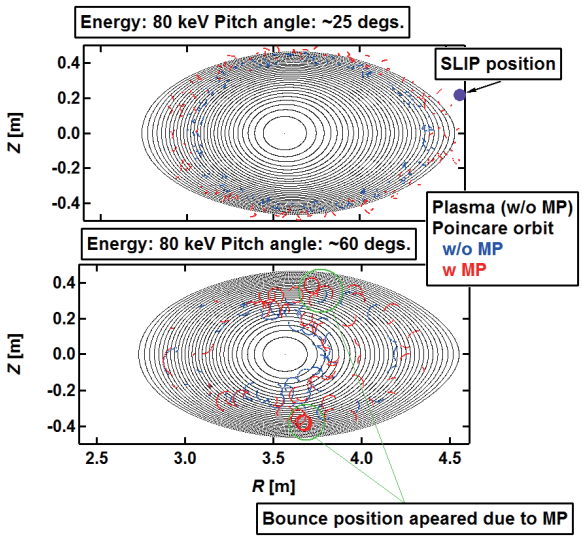

Fig. 5 Poincare plots of calculated Lorentz orbits of fast ions with (red) and without (blue) MPs at χ = 25° (top) and χ = 60° (bottom).

code [14]. In both figures, a bright spot occurs around E/χ of 20-180 keV/50°-70° during the NB injection; this corresponds to collisional losses [15]. Note that because of the energy resolution of SLIP (energy resolution at 180 keV is about 50 keV), the fast-ion loss is above the injection energy of NB (180 keV). The gain of the I.I. in the camera is the same, as shown in these pictures; the images suggest that static MPs increase fast-ion losses at wide E/χ ranges. Figure 4 shows the time evolution of fast-ion losses measured by PMT numbers 3 and 14. In Fig. 3, the regions surrounded by the black dashed circles locate the E and χ regions covered by each PMT. With static MP, fast-ion loss signals measured by SLIP having E/χ of 70~180 keV/55°~70° increase by 100%, whereas the fast-ion loss rate to SLIP having energy/pitch angle range of 70~180 keV/20°~40° increases by 50% with MP. We found that the effects of MPs on fast-ion loss signals measured by SLIP are clearly observed in both the high and low pitch-angle regions. For the discharge with static MPs, oscillations occurred in the fast-ion loss signal. This phenomenon is not yet completely understood, but the static MP may affect the stability of the marginal magnetohydrodynamics mode, which can induce loss of fast ions.

4. Orbit Calculations

To understand how such a small static MP affects a fast-ion orbit, the Lorentz orbits of fast ions were compared with and without static MPs. In this calculation, the Lorentz force equation for the motion of a charged particle ($m \cdot d\boldsymbol{v}/dt = q\ (\boldsymbol{v} \times \boldsymbol{B})$) was solved using a sixth order Runge-Kutta method for the LHD magnetic field in Cartesian coordinates. Here, m, v, t, q, and B represent the mass of a particle, the velocity of a particle, time, charge of particles, and magnetic field, respectively. We calculated the orbit from R = 3.05 m and Z = 0.0 m on a horizontally elongated cross section for 1 ms. Based on our experimental observations, we selected E/χ = 80 keV/25° and 80 keV/60°. Poincaré plots of the Lorentz orbits are shown in Fig. 5; the figure indicates that fast ions having χ = 25° have a co-going orbit, whereas those having χ = 60° have a transition orbit. Note that the transition orbit lies in the pitch angle region between the passing and helically trapped orbits. Due to MPs, the orbits of the co-going and transition ions move to the larger minor radius region of the plasma. Here, in the case of without static MPs, the width of the Poincaré plot corresponds to a Larmor diameter (~12 cm); however, with static MPs, the width of the Poincaré plot is larger than the Larmor diameter. This means that the orbit becomes stochastic because of static MPs. For transition ions, new bounce positions appear because of static MPs. These effects potentially enhance the transport or loss of fast ions, so fast-ion losses measured by SLIP can be increased by such a small static MP.

5. Summary

Using a scintillator-based lost fast-ion probe, we have studied the effects of MPs on fast-ion losses in the LHD. Energy and pitch-angle resolved measurements of fast-ion loss signals measured by SLIP show an increase in the fast-ion loss signal in the wide energy and wide pitch-angle regions. To understand the effects of MPs on fast-ion orbits, an orbit-following calculation was performed that included

the static MP field. The calculation indicates that a small static MP can change the orbits of fast ions (radial transport and stochastic orbit), which enhances the transport/loss of fast ions.

Acknowledgements

This work was partially supported by a Grant-in-Aid for Scientific Research from JSPS Nos. 21360457 and 21340175, and from the LHD project budget (NIFS13ULHH003). The authors are grateful to the LHD operation group for their excellent technical support. One of the authors (K. O.) would like to express the deepest appreciation to Y. Suzuki for his kind support in providing us the magnetic field data.

[1] A. Loarte *et al*., Nucl. Fusion **47**, S203 (2007).
[2] H. Zohm, Plasma Phys. Control. Fusion **38**, 105 (1996).
[3] P. Lang *et al*., Nucl. Fusion **53**, 043004 (2013).
[4] T. Hender *et al*., Nucl. Fusion **32**, 2091 (1992).
[5] T. Evans *et al*., Phys. Rev. Lett. **92**, 235003 (2004).
[6] Y. Liang *et al*., Phys. Rev. Lett. **98**, 265004 (2007).
[7] W. Suttrop *et al*., Phys. Rev. Lett. **106**, 225004 (2011).
[8] K. Toi *et al*., Nucl. Fusion **54**, 033001 (2014).
[9] K. Ogawa *et al*., Plasma Fusion Res. **3**, S1082 (2008).
[10] K. Ogawa *et al.*, J. Plasma Fusion Res. **8**, 655 (2009).
[11] K. Toi *et al.*, Plasma Phys. Control. Fusion **53**, 024008 (2011).
[12] I. Yamada *et al*., Fusion Sci. Tech. **58**, 345 (2010).
[13] T. Tokuzawa *et al*., Fusion Sci. Tech. **58**, 352 (2010).
[14] S. Zweben *et al*., Nucl. Fusion **30**, 1551 (1990).
[15] K. Ogawa *et al*., Plasma Fusion Res. **7**, 2402014 (2012).